BNL-203502-2018-JAAM

A New Strategy to Synthesize Anisotropic SmCo5 Nanomagnets

B. Shen, D. Su

To be published in "Nanoscale"

April 2018

Center for Functional Nanomaterials

Brookhaven National Laboratory

U.S. Department of Energy

USDOE Office of Science (SC), Basic Energy Sciences (BES) (SC-22)

DISCLAIMER

A New Strategy to Synthesize Anisotropic $SmCo_5$ Nanomagnets

Bo Shen,[a] Chao Yu,[a] Dong Su,[b] Zhouyang Yin,[a] Junrui Li,[a] Zheng Xi,[a] and Shouheng Sun*[a]

We report a simple strategy to synthesize anisotropic $SmCo_5$ nanoplates. The strategy involves the pre-synthesis of 125 x 12 nm $Sm(OH)_3$ nanorods and 10 nm Co nanoparticles followed by self-assembly of these nanorods and nanoparticles into $Sm(OH)_3$-Co nanocomposites. Once embedded in CaO matrix, the nanocomposite is subject to high temperature (850 °C) annealing in the presence of Ca, leading to the formation of 125 x 10 nm $SmCo_5$ nanoplates, which are dispersible in ethanol, allowing the alignment in epoxy resin under a 20 kOe magnetic field. The aligned $SmCo_5$ nanoplates show a square hysteresis behavior with room temperature coercivity reaching 30.1 kOe, which is among the highest values ever reported for $SmCo_5$ made from chemical methods. The work provides a new approach to high-performance anisotropic $SmCo_5$ for permanent magnet applications.

Introdiction

Developing nanomagnets that contain rare-earth metal alloys is an important step to maximize their magnetic performance for miniaturization of magnetic and electronic devices.[1-5] Among two classes of well-known rare earth magnets of Nd-Fe-B and Sm-Co, SmCo alloys, such as $SmCo_5$, are especially sought after for high temperature applications due to their large magnetocrystalline anisotropy constant (1.7 × 10^8 erg/cm^3) and high Curie temperature (747 °C).[6-10] Compared to isotropic $SmCo_5$ nanomagents, anisotropic $SmCo_5$ ones attract even more attention due to their square hysteresis behaviors and their capability of storing high magnetic energy densities.[11-12] However, fabrication of anisotropic $SmCo_5$ is a very challenging goal to reach thus far due to the difficulty in controlling the texture of nanosized $SmCo_5$ and the fast oxidation of Sm at the nanoscale. Previously, attempts to make anisotropic $SmCo_5$ by using ball milling, spark sintering, and spin melting, often yield microstructured magnets without showing the desired enhancement in magnetics.[13-16] Among these work, the best $SmCo_5$ made from ball milling following by annealing shows a coercivity of 41.5 kOe[14], but the size is around 280-400 nm, which is hard to be dispersed in solution and shows two phase behaviour hysteresis. Solution phase based chemical reduction methods have also been explored to prepare nanostructured $SmCo_5$, but they only lead to the formation of shape-isotropic $SmCo_5$.[17-21]

Herein, we report a new strategy to synthesize anisotropic $SmCo_5$ nanoplates that can be aligned magneically to show large magnetic coercivity. The method, illustrated in Fig. 1, includes the preparation of a nanocomposite of $Sm(OH)_3$ nanorods (NRs) and Co nanoparticles (NPs) via self-assembly, the coating of this nanocomposite with a protective CaO layer, and high temperature (850 °C) reduction of $Sm(OH)_3$-Co nanocomposite to obtain $SmCo_5$ nanoplates. With the Co NP size fixed at 10 nm, the right Sm/Co ratio is realized by controlling the NR dimension. These nanoplates (125 nm × 10 nm) could be suspended in ethanol and further mixed in epoxy resin. Under an external magnetic field of 20 kOe, these nanoplates can be aligned with the plates stacking along their crystallographic *c*-direction. The anisotropic $SmCo_5$ nanoplate assembly in epoxy resin has a square hysteresis behavior with its room temperature coercivity reaching 30.1 kOe, which is among the highest values ever reported for nanostructured $SmCo_5$. Our synthesis offers a promising new approach to the fabrication of anisotropic $SmCo_5$ nanomagnets for high performance permanent magnetic applications.

Experimental

Chemicals: The syntheses were carried out using standard airless procedures and commercially available reagents. Samarium chloride (99%), calcium acetylacetonate ($Ca(acac)_2$, 98%) and metallic Ca (99%) were purchased from Strem Chemicals. Hexadecyltrimethylammonium hydroxide (HTMA-OH, 25% in methanol) was purchased from TGI America. Cobalt carbonyl ($Co_2(CO)_8$), sodium hydroxide (98%), tetralin (1,2,3,4-tetrahydronaphthalen, 99%), 1-octadecene (ODE, 90%), oleylamine (OAm, 70%), dioctylamine (98%), oleic acid (90%) were from Sigma-Aldrich.

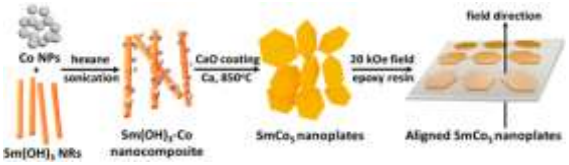

Fig. 1 Schematic illustration of the synthesis of anisotropic $SmCo_5$ nanoplates by self-assembly of $Sm(OH)_3$ NRs and Co NPs, followed by CaO coating and reductive annealing.

Synthesis of $Sm(OH)_3$ NRs: 0.42 g $SmCl_3$ was dissolved in a solution of 40 mL deionized water and 10 mL ethanol. The aqueous solution was heated to 90 °C and 10 mL of 2 M NaOH

[a] *Department of Chemistry, Brown University, Providence, Rhode Island 02912, United States*
[b] *Center for Functional Nanomaterials, Brookhaven National Laboratory, Upton, New York 11973, United States*

aqueous solution was added dropwise. After refluxed at 90 °C for 5 h, the solution was cooled to room temperature and the product was collected by centrifugation (8000 rpm, 8 min). The white precipitate, $Sm(OH)_3$ NRs, was further washed with deionized water and dried at room temperature.

Synthesis of Co NPs: A mixture of 17 mL tetralin, 0.35 mL of oleic acid and 0.5 mL of dioctylamine in a four-neck flask was heated to 120 °C under argon flow for 1 h. Then the solution was heated up to 210 °C. Under a blanket of argon, a solution of 0.27 g $Co_2(CO)_8$ dissolved in 3 mL tetralin was injected and the solution was kept at 210 °C for 30 min. The solution was then cooled to room temperature and black NPs were collected by the addition of ethanol and subsequent centrifugation (8500 rpm, 8 min). The solid product was dispersed in hexane (15 mL) and precipitated by adding ethanol (20 mL) and by centrifugation. The Co NPs were re-dispersed in hexane for further use.

Synthesis of $Sm(OH)_3$-Co composite: To prepare $Sm(OH)_3$-Co composite, 0.02 g of $Sm(OH)_3$ NRs were suspended in 20 mL hexane under sonication. 0.027 g of Co NPs dispersed in 10 mL of hexane was added to the $Sm(OH)_3$ suspension dropwise under sonication. After 3 h of sonication, hexane dispersion was obtained and the $Sm(OH)_3$-Co composite was collected by adding ethanol (20 mL) and centrifugation (8500 rpm, 8 min). The solid product was measured by ICP-AES to have a Sm/Co mass ratio of 1:4.5 and was re-dispersed in hexane for further uses.

Coating $Sm(OH)_3$-Co composite with CaO: 0.5 g $Ca(acac)_2$, 20 mL ODE, 1 mL oleic acid and 1 mL oleylamine were mixed in a flask under magnetic stirring. The solution was heated to 100 °C under argon and kept at this temperature for 30 min. Then 0.1 g $Sm(OH)_3$-Co (prepared from repeated synthesis due to the amount of hexane (30 mL) used in each synthesis) was added to the solution. After 10 min, 8 mL methanol solution of HTMA-OH was added into the solution dropwise. The mixture was kept at 100 °C for 30 min to remove methanol. Then the solution was heated to 150 °C and kept at 150 °C for 1 h before it was cooled to room temperature. The $Sm(OH)_3$-Co/CaO composite was precipitated by adding ethanol (20 mL) followed by centrifugation (8500 rpm, 8 min). The precipitate was washed twice with ethanol (2 x 40 mL) and hexane (2 x 10 mL) and then dried for further annealing. As we saw no loss of Sm and Co during the coating process, we should still have 0.1 g of $Sm(OH)_3$-Co in the CaO matrix.

Synthesis of anisotropic $SmCo_5$ nanoplates: All processes were done under argon. 0.3 g $Sm(OH)_3$-Co embedded in CaO was ground with 0.3 g metallic Ca in the stainless-steel boat. Then the mixture was heated under an argon atmosphere to 850 °C at a rate of 25 °C/min and kept at 850 °C for 30 min. After cooled to room temperature, the powder was washed with deionized water to remove CaO and excess Ca. Then the powder was milled in 10 mL ethanol in the presence of 0.1 mL oleic acid for 1 h to form a dispersion (note: in the synthesis of Co NPs described above, oleate-coated Co NPs were dispersed in hexane, but here, $SmCo_5$ nanoplates were dispersible in ethanol, suggesting the formation of a bilayer coating of oleate with hydrocarbon chains intercalated.). The undispersed was removed by centrifugation (100 rpm, 10 seconds), and the product in the dispersion was collected by a bar magnet and dried, giving 0.08 g $SmCo_5$ nanoplates for further uses.

Embedding $SmCo_5$ nanoplates in epoxy resin and magnetic alignment: All processes were done under argon. First, 0.2 g epoxy resin was dissolved in 2 mL ethanol to form a clear solution. Then 0.2 g $SmCo_5$ nanoplates (obtained from the repeated syntheses due to the volume constraint of the stainless-steel boat we used) in 2 mL ethanol dispersion was added dropwise into the resin solution under sonication to obtain a homogenous $SmCo_5$-resin solution. After ethanol evaporation, the resin gel was pasted on the surface of a TEM grid or a silicon substrate. The TEM grid or silicon substrate were put in a 20 kOe field until the resin was solidified. For the TEM grid, the external magnetic field was set parallel to the grid surface. For the silicon substrate, the external magnetic field was set perpendicular to the substrate surface for XRD and magnetic property measurements.

Characterization: TEM images and High-resolution TEM (HRTEM) images were obtained on a JEOL 2010 TEM at 200 kV. High-angle annular dark-field scanning transmission electron microscopy (HAADF-STEM) and STEM-electron energy-loss spectroscopy (STEM-EELS) elemental mapping were collected from a Hitachi HD2700C (200 kV) to characterize the elemental distribution of the nanoplates. Powder XRD patterns of the $SmCo_5$ nanoplates were recorded on a Bruker AXS D8-Advanced diffractometer with CuKa radiation (λ = 1.5418 Å). The Sm/Co composition was determined by elemental analysis using a JY2000 Ultrace ICP Atomic Emission Spectrometer. Magnetic properties were measured on a Physical Property Measurement System (PPMS) under a maximum applied field of 90 kOe.

Result and discussion

Monodisperesed 10 (± 1) nm Co NPs were obtained by decomposition of $Co_2(CO)_8$ in tetralin solution of dioctylamine and oleic acid (Fig. 2a).[22] The X-ray diffraction (XRD) shows the Co NPs have a crystalline face centered cubic (*fcc*) structure (Fig. 2b). Separately, $Sm(OH)_3$ NRs were prepared in aqueous solution. It was important here to control NR aspect ratio to obtain the correct Sm/Co ratio. For example, if $Sm(OH)_3$ NRs were prepared by precipitating aqueous solution of $SmCl_3$ with 2 M NaOH at 100 °C as we described previously,[18] we could only obtain 60 x 15 nm $Sm(OH)_3$ NRs that were unsuitable for the formation of $Sm(OH)_3$-Co composites with the right 1/5 Sm/Co ratio. In the current synthesis, we still used 2 M NaOH to precipitate $SmCl_3$, but the reaction was controlled in a mixture solution (40 ml deionized water and 10 ml ethanol) at 90 °C (refluxing) for 5 h, which yielded 125 (± 25) nm × 12 (± 3) nm $Sm(OH)_3$ NRs (Fig. 2c). The hexagonal $Sm(OH)_3$ structure was confirmed by X-ray diffraction (XRD) (Fig. 2d). The $Sm(OH)_3$ NRs obtained from our current new synthesis have a higher aspect ratio (about 10), allowing to accomodate more Co NPs to reach the desired Sm/Co ratio close to 1/5.

The hexane dispersion of Co NPs were added dropwise to a suspension of $Sm(OH)_3$ NRs in hexane at a controlled molar

ratio (Sm:Co = 1:4.5 for the synthesis of $SmCo_5$). After 3 hours of sonication, the $Sm(OH)_3$-Co nanocomposite was obtained (Fig. 3a). The rod-like nanocomposite work as the precursor for the reductive annealing. We should emphasize that the anisotropic feature of $Sm(OH)_3$ NRs and the Co NP attachment to the NRs is essential for the formation of $SmCo_5$ nanoplates from the next step reduction procedure. Other combinations of $Sm(OH)_3$ NRs and $Co(OH)_2$, including $Co(OH)_2$ matrix coating over $Sm(OH)_3$ NRs, could only yield shape-isotropic $SmCo_5$ without good control on nanostructures (Fig. S1). Nanostructured $SmCo_5$ was obtained by high temperature (850 °C) annealing of $Sm(OH)_3$-Co nanocomposite embedded in CaO in the presence of Ca. Here CaO was specifically chosen for the $SmCo_5$ stabilization need because of following benefits: 1) CaO is thermally very stable, having a high melting point (above 2500 °C); 2) CaO is compatible with the Ca reduction process, which also leads to the formation of CaO; 3) CaO can be removed easily by water washing, facilitating $SmCo_5$ product purification. In the experiment, we mixed the nanocomposite with $Ca(acac)_2$ and HTEMA-OH in 1-octadecene and heated the solution at 150 °C for 1 h to allow the decomposition of $Ca(acac)_2$ to CaO. Fig. 3b shows a representative TEM image of the $Sm(OH)_3$-Co nanocomposite embedded in the CaO matrix. Inductively coupled plasma-atomic emission spectroscopy (ICP-AES) analysis confirmed that the CaO coating process had no effect on Sm/Co composition. After drying the powder in air, we ground the $Sm(OH)_3$-Co/CaO nanocomposite with Ca under an argon atmosphere and annealed the mixture at 850 °C. We

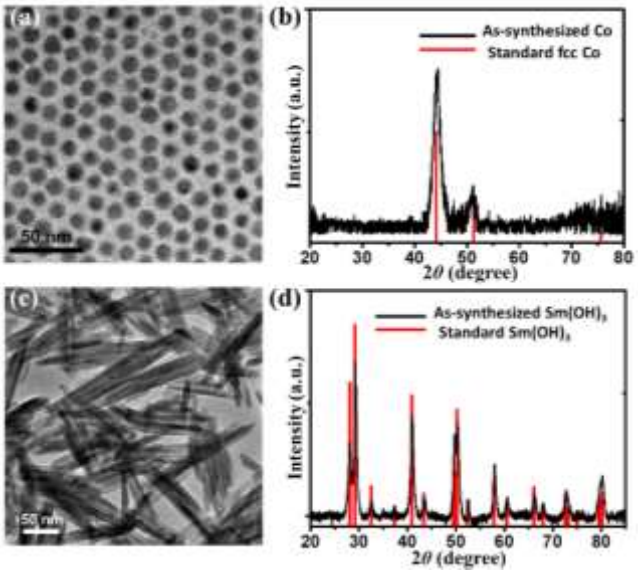

Fig. 2 (a) TEM image of the as-synthesized 10 nm Co NPs. (b) XRD of the as-prepared Co NPs (black curve) and the standard *fcc*-Co (red lines, JPCDS No. 15-0806). (c) TEM image of 125 x 12 nm $Sm(OH)_3$ NRs. (d) XRD of the as-prepared $Sm(OH)_3$ NRs (black curve) and the standard pattern of $Sm(OH)_3$ (red lines, JPCDS No. 83-2036).

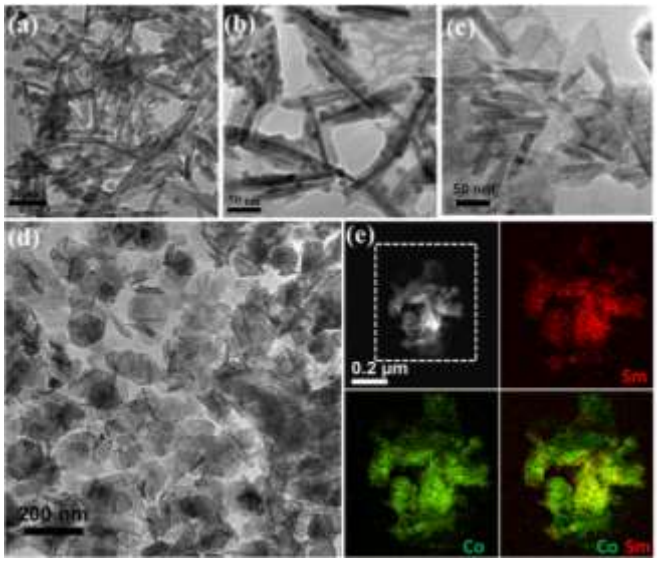

Fig. 3 (a) TEM image of $Sm(OH)_3$-Co nanocomposite with Sm:Co =1:4.5 (molar ratio). (b) TEM image of $Sm(OH)_3$-Co nanocomposite embedded in CaO matrix. (c) TEM image of $Sm(OH)_3$-Co nanocomposite obtained 10 min after the annealing. (d) TEM image of the as-synthesized $SmCo_5$ nanoplates. (e) HAADF-STEM and elemental mapping of the $SmCo_5$ nanoplates, showing the formation of uniform alloy structure within each nanoplate.

monitored the annealing process by sampling and characterizing a small amount of the annealed product by TEM at different times. 10 min after the annealing, Co NPs started to diffuse into the $Sm(OH)_3$ NRs (Fig. 3c). After 30 min annealing, $SmCo_5$ nanoplates were formed. Once cooled to room temperature, the powder was washed with distilled water under argon to remove CaO and any unconsumed reactants. After washing, the powder was ground in ethanol and formed a dispersion. A gentle centrifugation (100 rpm) was applied to remove a small amount of precipitate from the dispersion, then the product was collected from the dispersion by a bar magnet. The product had a final Sm/Co composition of 1:5 as analyzed by ICP-AES, which is reduced from the original 1:4.5, suggesting a small Sm loss during the annealing and washing processes. Fig. 3d shows the TEM image of the as-synthesized $SmCo_5$ nanoplates with their hexagon-like lateral dimension in 125 ± 25 nm and thickness around 10 ± 5 nm. The chemical composition of the nanoplates was further characterized with HAADF-STEM analysis and STEM-EELS elemental mapping (Fig. 3e). The elemental distribution confirms the presence of Sm (red) and Co (green) across the nanoplate, and the combined (green and red) image shows Sm and Co elements are homogeneously distributed in the nanoplates, indicating that the nanoplates have a uniform $SmCo_5$ alloy structure.

The detailed structure of the nanoplate was analyzed by HRTEM image. Fig. 4a is a plane-view HRTEM image of a representative nanoplate. The distance of the lattice fringe was measured to be 2.15 Å that is close to the lattice spacing of (200) planes of the hexagonal $SmCo_5$ (2.16 Å). The fast Fourier transform (Fig. 4b) pattern obtained from Fig. 4a matches with the simulated electron diffraction pattern (Fig.

4c) along [001] zone axis of a hexagonal phase of the $SmCo_5$ (P6/mmm). The atomic arrangement of the nanoplate revealed by HRTEM (Fig. 4d) shows the same Sm, Co periodicity as that from an atom model built along [001] zone axis of $SmCo_5$ crystal lattice (Fig. 4e). All these analyses support that the *c*-axis of the $SmCo_5$ nanoplate is perpendicular to the hexagonal plane. HRTEM image of the side-view of a nanoplate (Fig. 4f) show two kinds of lattice fringes with their interfringe distances at 2.48 Å and 1.99 Å, which correspond to lattice spacing of (110) planes (2.49 Å) and (002) planes (1.98 Å) of $SmCo_5$ respectively. Such image agrees well with the simulated atom model along [1, -1, 0] zone axis of $SmCo_5$ crystal lattice (Fig. 4g). The further supports that the *c*-axis is perpendicular to the plane of the $SmCo_5$ nanoplate.

XRD peaks of the nanoplate powder confirm that the nanoplates have the crystalline hexagonal D_{2d} structure of $SmCo_5$ (Fig. 5a). The pattern intensity fits well with the standard $SmCo_5$, indicating that the nanoplates in the powder form have no preferred texture. The powder was strongly ferromagnetic at room temperature with its coercivity (H_c) and saturation magnetization (M_s) values at 25.3 kOe and 52.5 emu/g, respectively (Fig. 5b). The M_s value is reduced from the bulk $SmCo_5$ value (99 emu/g) due to surface coating of oleate (for forming the nanoplate dispersion) and the related nanoscale surface effects, which is consistent with what have been observed on nanostructured $SmCo_5$.[23, 24]

The dispersible $SmCo_5$ nanoplates in ethanol made it possible to align them under a magnetic field. To demonstrate this point, we first tested the assembly during ethanol evaporation in a 20 kOe magnetic field, and found that the sample was only partially aligned (Fig. S2). We then mixed the $SmCo_5$ nanoplates and epoxy resin in ethanol at the mass ratio of 1:1. After ethanol evaporation, the $SmCo_5$ nanoplates were embedded in epoxy resin, and aligned in the same 20 kOe field before the resin was hardened, as indicated in Fig. 6a. As the *c*-axis of each of the nanoplates is also its magnetic easy axis direction, the aligned $SmCo_5$ nanoplates should stack face-to-face along the field direction. From the TEM images (Fig. 6b), we can see that the

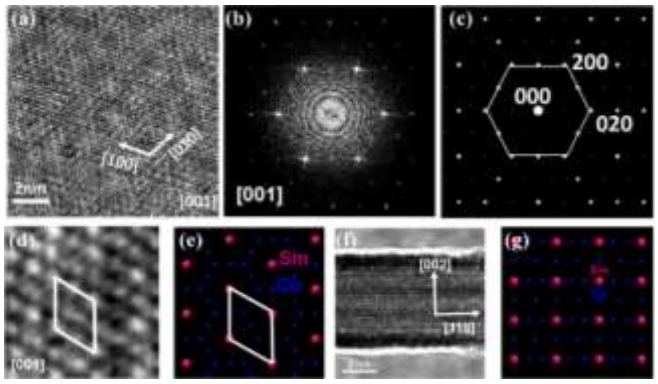

Fig. 4 (a) HRTEM image of a part of one $SmCo_5$ nanoplate (planar view). (b) Fast Fourier transform pattern of (a). (c) Simulated SAED pattern of hexagonal $SmCo_5$ projected along the *c*-axis. (d) A fraction of HRTEM imaging area in showing the arrangement of Sm and Co atoms. (e) Modeled hexagonal $SmCo_5$ structure projected along the *c*-axis. (f) HRTEM image of the side-view of a $SmCo_5$ nanoplate. (g) Modeled $SmCo_5$ structure projected along [1, -1, 0].

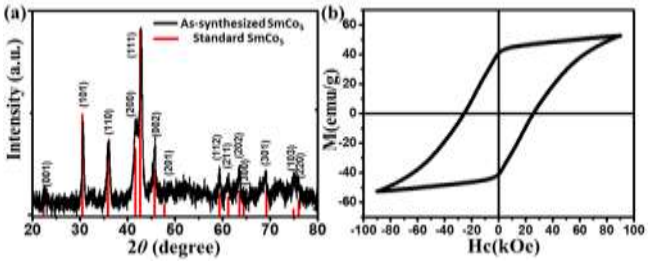

Fig. 5 (a) XRD of the as-synthesized $SmCo_5$ nanoplate powder (black curve) and the standard pattern of D_{2d} structure $SmCo_5$ (red lines, JPCDS No. 65-8981). (b) hysteresis loop of the as-synthesized $SmCo_5$ nanoplate powder measured at 300 K.

$SmCo_5$ nanoplates are aligned along the external field direction with a face-to-face arrangement. Furthermore, we measured the XRD diffraction patterns and used the relative intensity ratio between the diffraction peaks of (002) and (111), $I_{(002)}/I_{(111)}$, to measure the alignment factor (The intensity ratio is 0.26 for an isotropic $SmCo_5$ sample).[17] As shown in Fig. 6c, the non-aligned $SmCo_5$ nanoplates give the $I_{(002)}/I_{(111)}$ ratio of 0.4, suggesting that there is some degree of alignment in the powder product due likely to the nanoplate shape effect. After magnetic field alignment, the (111) peak nearly disappears and the $I_{(002)}/I_{(111)}$ ratio increases to 20, indicating a strong texture with the $SmCo_5$ nanoplates parallel to the substrate. These aligned nanoplates show obvious anisotropic magnetic hysteresis behavior at room temperature - the out-of-plane loop is square (H_c = 30.1 kOe and M_s = 66.1 emu/g) while the in-plane one is minor, showing no M_s at a 90 kOe field (Fig. 6d). The measured H_c (30.1 kOe) from the aligned nanoplate assembly is among the highest values ever reported for nanostructured $SmCo_5$.[17-21, 23-26] The magnetic

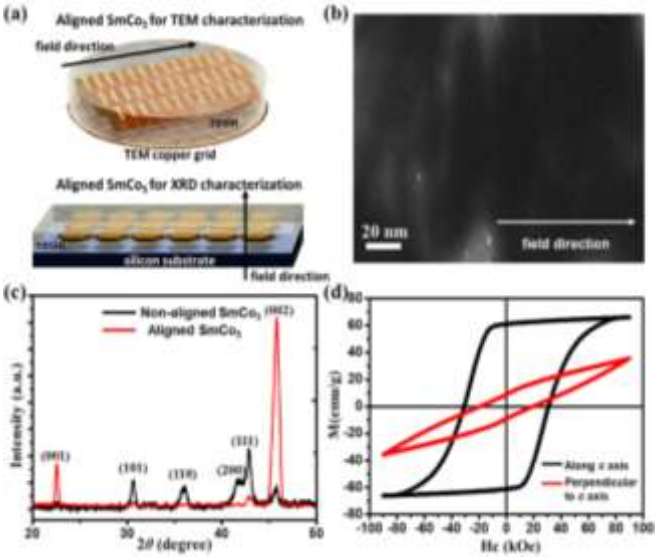

Fig. 6 (a) Schematic illustration of $SmCo_5$ nanoplate alignment in resin along the magnetic field direction for TEM and XRD characterizations. (b) TEM image of the aligned $SmCo_5$ nanoplates embedded in resin. (c) XRD patterns of the non-aligned $SmCo_5$ (black curve) and the aligned

$SmCo_5$ nanoplates (red curve). (d) Room temperature hysteresis loops of the aligned $SmCo_5$ nanoplates measured along the *c* axis (black curve) and perpendicular to the *c* axis (red curve).

alignment factor can be quantitatively measured by the remanence ratio (m_r), which is defined as M_r/M_s, (M_r is the remanence along the aligned direction).[27-29] For a group of Stoner-Wohlfarth type particles, this remanence ratio is 0.5 for the randomly oriented particles but 1 for a perfectly aligned particle assembly.[30] Practically, the larger the m_r, the better the magnetic alignment. The loop from the aligned $SmCo_5$ nanoplates in Fig. 6d has m_r = 0.92, which is among the highest values ever reported,[8,11,12,30] indicating a high anisotropic order of the $SmCo_5$ nanoplates in resin.

Conclusions

In summary, we have reported a novel method to synthesize dispersible $SmCo_5$ nanoplates and to align them in resin to obtain anisotropic nanoplate assemblies. The key process is first to assemble 10 nm Co NPs along 125 nm × 12 nm $Sm(OH)_3$ NRs and then to embed the $Sm(OH)_3$-Co nanocomposite in CaO matrix for high temperature (850 °C) annealing in the presence Ca. The CaO coating ensures Co diffusion and alloying with Sm in the annealing condition, and the NR shape facilitates the formation of 125 × 10 nm $SmCo_5$ nanoplates. An important feature of these nanoplates is that they can be dispersed in ethanol and therefore, be assembled in resin under a magnetic field to allow the $SmCo_5$ nanoplates to stack face-to-face, establishing the desired anisotropic texture and magnetic alignment. The aligned anisotropic $SmCo_5$ nanoplates have a square hysteresis loop with a room temperature H_c of 30.1 kOe that is among the largest coercivity values ever reported for $SmCo_5$. With the $Sm(OH)_3$ NR dimension and Co NP size controls, $SmCo_5$ nanoplate dimensions should in principle be further tuned to achieve optimum magnetic performance. The dispersion nature of these nanoplates should also allow assembly of $SmCo_5$ with other high moment magnetic NPs of Co, Fe, or FeCo, making it possible to fabricate anisotropic $SmCo_5$-M (M = Co, Fe, or FeCo) exchange-coupled nanocomposites with optimum magnetics for high performance permanent magnet applications.

Conflicts of interest

There are no conflicts to declare.

Acknowledgements

This work was supported by the Critical Materials Institute, an Energy Innovation Hub funded by the U.S. Department of Energy, Office of Energy Efficiency and Renewable Energy, Advanced Manufacturing Office. Part of electron microscopy work was carried out at the Center for Functional Nanomaterials, Brookhaven National Laboratory (BNL), which is supported by the DOE, Office of Basic Energy Sciences, under contract DE-SC-0012704.

Notes and references

1 R. Skomski, J. M. D. Coey, *Phys. Rev. B* 1993**, 48**, 15812-15816.
2 F. Liu, Y. Hou, S. Gao, *Chem. Soc. Rev.* 2014**, 43**, 8098-8113.
3 D. J. Sellmyer, *Nature* 2002, **420**, 374-375
4 W. B. Cui, Y. K. Takahashi, K. Hono, *Adv. Mater.* 2012**, 24**, 6530-6535.
5 M. Yue, X. Zhang, J. P. Liu, *Nanoscale* 2017, **9**, 3674-3697.
6 S. Sun, C. B. Murray, D. Weller, L. Folks, A. Moser, *Science* 2000, **287**, 1989-1992.
7 Z. Zhang, X. Song, Y. Qiao, W Xu, J. Zhang, M. Seyring, M. Rettenmayr, *Nanoscale*, 2013, **5**, 2279-2284
8 S. Sawatzki, R. Heller, C. Mickel, M. Seifert, L. Schultz, V. Neu, *J. Appl. Phys.* 2011**, 109**, 123922.
9 C. H. Chen, S. J. Knutson, Y. Shen, R. A. Wheeler, J. C. Horwath, P. N. Barnes, *Appl. Phys. Lett.* 2011**, 99**, 012504.
10 M. Seyring, X. Song, Z. Zhang, M. Rettenmayra, *Nanoscale*, 2015, **7**, 12126-12132
11 W. L. Zuo, X. Zhao, J. F. Xiong, M. Zhang, T. Y. Zhao, F. X. Hu, J. R. Sun, B. G. Shen, *Sci. Rep.* 2015**, 5**, 13117
12 C. B. Rong, V. V. Nguyen, J. P. Liu, *J. Appl. Phys.* 2010, **107**, 09A717.
13 L. Zheng, B. Cui, N. G. Akdogan, W. Li, G. C. Hadjipanayis, *J. Alloys. Compd.* 2010, **504**, 391-394.
14 A. M. Gabay, X. C. Hu, G. C. Hadjipanayis, *J. Magn. Magn. Mater.* 2014**, 368**, 75-81.
15 M. Yue, J. H. Zuo, W. Q. Liu, W. C. Lv, D. T. Zhang, J. X. Zhang, Z. H. Guo, W. Li, *J. Appl. Phys.* 2011**, 109**, 07A711.
16 A. R. Yan, W. Y. Zhang, H. W. Zhang, B. G. Shen, *J. Magn. Magn. Mater.* 2000**, 210**, L10-L14
17 Y. Hou, Z. Xu, S. Peng, C. B. Rong, J. P. Liu, S. Sun, *Adv. Mater.* 2007**, 19**, 3349-3352.
18 B. Shen, A. Mendoza-Garcia, S. E. Baker, S. K. McCall, C. Yu, L. Wu, S. Sun, *Nano Lett.* 2017, **17**, 5695-5698.
19 Z. Ma, T. Zhang, C. Jiang, *Chem. Eng. J.* 2015**, 264**, 610-616.
20 C. Yang, L. Jia, S. Wang, C. Gao, D. Shi, Y. Hou, S. Gao, *Sci. Rep.* 2013, **3**, 3542.
21 G. S. Chaubey, N. Poudyal, Y. Liu, C. B. Rong, J. P. Liu, *J. Alloys. Compd.* 2011**, 509**, 2132-2136.
22 L. Wu, Q. Li, C. H. Wu, H. Zhu, A. Mendoza-Garcia, B. Shen, J. Guo, S. Sun, *J. Am. Chem. Soc.* 2015, **137**, 7071-7074.
23 H. W. Zhang, S. Peng, C. B. Rong, J. P. Liu, Y. Zhang, M. J. Kramer, S. H. Sun, *J. Mater. Chem.* 2011, **21**, 16873-16876.
24 Z. Ma, T. Zhang, C. Jiang, *RSC Adv.* 2015, **5**, 89128-89132.
25 D. W. Hu, M. Yue, J. H. Zuo, R. Pan, D. T. Zhang, W. Q. Liu, J. X. Zhang, Z. H. Guo, W. Li, *J. Alloys Compd.* 2012, **538**, 173-176.
26 Z. Ma, S. Yang, T. Zhang, C. Jiang, *Chem. Eng. J.* 2016, **304**, 993-999.
27 F. Wang, H. Wei, L. Liu, H. Yang, J. Zhang, J. Du, W. Xia, A. Yan, J. P. Liu, *J. Appl. Phys.* 2015, **117**, 17D142.
28 X. Li, L. Lou, W. Song, Q. Zhang, G. Huang, Y. Hua, H. Zhang, J. Xiao, B. Wen, X. Zhang, *Nano Lett*. 2017, **17**, 2985–2993.
29 B. Balasubramanian, B. Das, R. Skomski, W. Y. Zhang, D. J. Sellmyer, *Adv. Mater.* 2013, **25**, 6090-6093.
30 L. Liu, S. Zhang, J. Zhang, J. P. Liu, W. Xia, J. Du, A. Yan, J. Yi, W. Li, Z. Guo, *J. Magn. Magn. Mater.* 2015, **374**, 108-115.